DEFORMATION DUE TO DIP-SLIP AND TENSILE FAULTS IN FORCE–LIKE IMPERFECTLY BONDED ELASTIC HALF-SPACES

Agin Kumari
Department of Mathematics, Chaudhary Bansi Lal University
Bhiwani-127021, India, Email: agincblu@gmail.com

Dinesh Kumar Madan (Corresponding Author)
Department of Mathematics, Chaudhary Bansi Lal University
Bhiwani-127021, India, Email: dk_madaan@rediffmail.com

ABSTRACT

Analytic expressions for stresses and displacements caused by two-dimensional seismic sources for imperfectly joined semi-infinite elastic half spaces having force-like interface are obtained. In the present paper, we have studied the effect of force-like imperfect interface on transmission of stresses across the interface of two joined elastic half spaces. The cases of vertical dip-slip and tensile fault are discussed in detail. Variations in stresses, for different imperfect bonding conditions of force-like and for perfect bonding, are depicted through graphs and mesh grids, using dimensionless approach. A significant influence of force-like imperfect interface on dislocation field due to dip-slip and tensile fault is observed.

KEYWORDS: Deformation; Tensile Fault; Perfect Interface; Force-Like Interface; Mesh Grids; Contours

INTRODUCTION

Interface modeling has been the focus of several studies related to theory of dislocations. A number of researchers studied the effect of different kind of imperfect interfaces on deformation field and introduced different interfacial models like smooth-bond, rigid-bond, dislocation-like, force-like etc. to simulate the real behavior at interfaces. As the interfaces are rarely perfect and the meticulous theoretical modeling is very difficult. The presence of imperfection at the interface influence the continuity of displacements and stresses. At a perfect interface displacement and stress are continuous across the interface; in imperfect interfaces displacements and stresses are no longer continuous.

Dunders and Hete´nyi [1] derived elastic solutions in rapports of the Papkovich-Neuber displacement function for a intense force near a smooth interface of two semi- infinite solids. Singh and Garg [2] derived solutions for 2-D seismic sources causing plane strain deformation. Singh et al. [3] computed analytic expressions for the displacements and stresses for two homogeneous, isotropic, perfectly elastic half-spaces having perfect interface produced by several two-dimensional seismic sources.

Yu [4] introduced dislocation-like interface modeling and obtained the Green's function and dislocations in a bimaterial. Fan and Wang [5] formulated the problem of imperfect interface modeling of a screw dislocation.

Displacements and stresses in layered half-space due to a long tensile fault present in the layer are found by Singh and Singh [6]. Kumar et al. [7] obtained the Airy stress function for a tensile line source in two perfectly joined half-spaces. Singh et al. [8] obtained static deformation for monoclinic elastic medium, using the eigenvalue approach. Bala and Rani [9] derived expressions for static deformation due to a very long buried dip-slip fault in an isotropic half-space perfectly joined with an orthotropic half-space.

Chu et al. [10] studied the displacement and stress fields due to a dislocation loop in a bimaterial system. Wu et al. [11] considered dislocation-like and force-like interfaces to obtain dislocation field in a bimaterial system. Kumari and Madan [12] has obtained analytic expressions for static deformation generated by vertical dip-slip fault in two imperfectly joined mediums having dislocation-like interface. Madan and Kumari [13] has drawn results for static deformation generated by vertical tensile fault in two half-spaces having dislocation-like bonding between them.

In dislocation-like interfaces, Stresses are continuous across the interface but displacements are not. In force-like interfaces the state is vice-versa i.e. displacements are continuous across the interface but stresses

are not. In fact, dislocation-like interfaces are all possible interfaces between the perfect and rigid interfaces and force-like interfaces are all possible interfaces between the perfect and traction-free interfaces.

In the present paper, a force-like imperfect interface model is applied to study the behavior of displacements and stresses across the interface. we have studied the effect of force–like imperfect interface on transmission of stresses across the interface of two imperfectly linked semi-infinite elastic half spaces. Following the work of Singh et al. [3], We have obtained analytic expressions for displacements and stresses caused by 2-Dimensional seismic sources (Centre of dilatation, Centre of rotation, single couple, double couple, dipole, long dip-slip dislocation) by applying force-like imperfect interface bonding conditions. Particular cases of vertical dip-slip and tensile faults caused by a line source are discussed in detail. Variations in stresses and discontinuity in stresses at the interface for different force-like imperfect bonding conditions are depicted through graphs and mesh grids, using dimensionless approach. Due to imperfection at interface, a jump discontinuity in stresses at interface is observed, the results were discussed numerically with the help of graphs, 3-D mesh grids with contour lines. A significant influence of force-like imperfect interface on dislocation field is seen.

BASIC THEORY

Two semi-infinite solids (homogeneous, isotropic, perfectly elastic) force-like imperfectly joined at the interface ($z = 0$) are considered. Cartesian co-ordinates are denoted by (x, y, z) and z-axis is taken vertically downward (Figure 1). We have considered a plain-strain problem; displacements $u_1 = 0$, u_2 and u_3 depends on y and z only. Upper half space ($z<0$) is termed as Medium-I & lower half space ($z>0$) is termed as Medium-II; λ_1, μ_1 and λ_2, μ_2 be elastic constants for Medium-I and II respectively. Following the results of Singh et al. [3] for a line source embedded in the Medium-II parallel to the x-axis passing through the point ($0, 0, \xi$) and $\xi>0$. Airy's stress function for Medium-I &II are,

$$U^{(I)} = \int_0^\infty [(L_1 + M_1 kz) \sin ky + (P_1 + Q_1 kz)\cos ky] k^{-1}\exp(kz)dk \qquad (1)$$

$$U^{(II)} = U_0 + \int_0^\infty [(L_2 + M_2 kz) \sin ky + (P_2 + Q_2 kz)\cos ky] k^{-1}\exp(-kz)dk \qquad (2)$$

where

$$U_0 = \int_0^\infty [(L_0 + M_0 k|z - \xi|) \sin ky + (P_0 + Q_0 k|z - \xi|)\cos ky] k^{-1}\exp(-k|z - \xi|)dk \qquad (3)$$

Superscript (I), (II) stands for Medium-I & II; L_i, M_i, P_i, Q_i, for $i = 1, 2$ are unknown, values of these are to be calculated from the force-like bonding conditions at interface $z = 0$; the source coefficients L_0, M_0, P_0 and Q_0 are free of variable k, values of these are given by Singh and Garg [2] and are reproduced as Table 1 in Appendix-I for ready reference.
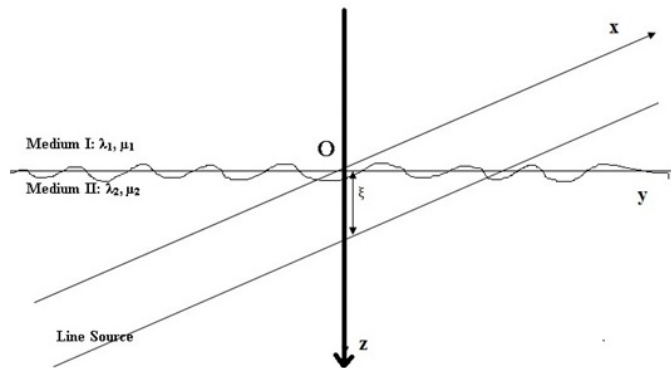

Fig. 1 Two half-spaces having force-like imperfect interface embedded a line source in the medium-II at ($0, 0, \xi$)

FORCE-LIKE INTERFACE MODELING AND ITS SOLUTION

For two half spaces having force-like imperfect bonding conditions at the interface at $z = 0$, are given by Wu et al. [11];

$$u_i^{(I)}|_{z^-=0} = u_i^{(II)}|_{z^+=0} \tag{4}$$

$$\tau_{i3}^{(I)}|_{z^-=0} = [k_{ij}]\tau_{j3}^{(II)}|_{z^+=0} \tag{5}$$

$i = 2, 3$;

where the constant matrix $[k_{ij}]$, describes imperfect interface bonding conditions at the boundary $z = 0$ plane. Matrix $[k_{ij}]$ is supposed to be diagonal and values of the matrix elements lies in the range (0, 1). The first element will be associated to interface conditions in the tangential direction, and the second element will be related to interface conditions in the normal directions. When all the diagonal entries of the matrix assume value 1, then interface conditions becomes perfect i.e. stresses and displacements become continuous across interface and if all diagonal entries assume value 0, then interface becomes stress-free i.e. the case when upper half-space is sliding over lower half-space. In fact, these conditions actually stand for all possible intermediate interface conditions between perfect and traction-free interface bonding conditions. Interfacial conditions in the tangential and normal directions are associated with the first and second element on the diagonal of the matrix respectively. The source coefficients L_0, M_0, P_0, Q_0 have different values for $z<\xi$ & $z>\xi$. Let L^-, M^-, P^-, Q^- be the values of L_0, M_0, P_0, Q_0 for $z<\xi$.

Firstly, we have derived integral expressions for displacements and stresses from (1) and (2) and then applying bonding conditions (4) and (5) to these expressions; we obtained,

$$A\begin{bmatrix} L_1 \\ M_1 \\ L_2 \\ M_2 \end{bmatrix} = \begin{bmatrix} k_{33}(L^- + M^- k\xi)\exp(-k\xi) \\ k_{22}(L^- - M^- + M^- k\xi)\exp(-k\xi) \\ \beta\left(L^- - \frac{M^-}{\alpha_2} + M^- k\xi\right)\exp(-k\xi) \\ \beta\left(L^- - M^- + \frac{M^-}{\alpha_2} + M^- k\xi\right)\exp(-k\xi) \end{bmatrix} \tag{6}$$

$$A\begin{bmatrix} P_1 \\ Q_1 \\ P_2 \\ Q_2 \end{bmatrix} = \begin{bmatrix} k_{33}(P^- + Q^- k\xi)\exp(-k\xi) \\ k_{22}(P^- - Q^- + Q^- k\xi)\exp(-k\xi) \\ \beta(P^- - Q^-/\alpha_2 + Q^- k\xi)\exp(-k\xi) \\ \beta(P^- - Q^- + Q^-/\alpha_2 + Q^- k\xi)\exp(-k\xi) \end{bmatrix} \tag{7}$$

where

$$A = \begin{bmatrix} 1 & 0 & -k_{33} & 0 \\ 1 & 1 & k_{22} & -k_{22} \\ 1 & 1/\alpha_1 & -\beta & -\beta/\alpha_2 \\ 1 & 1-1/\alpha_1 & \beta & \beta(1-1/\alpha_2) \end{bmatrix}$$

and

$$\alpha_1 = \frac{\lambda_1 + \mu_1}{\lambda_1 + 2\mu_1}, \alpha_2 = \frac{\lambda_2 + \mu_2}{\lambda_2 + 2\mu_2}, \ \beta = \frac{\mu_1}{\mu_2} \tag{8}$$

On solving equations (6) and (7), we get

$$\begin{bmatrix} L_1 \\ M_1 \\ L_2 \\ M_2 \end{bmatrix} = B\begin{bmatrix} L^- \exp(-k\xi) \\ M^- \exp(-k\xi) \\ M^- kc \exp(-k\xi) \end{bmatrix} \quad and \quad \begin{bmatrix} P_1 \\ Q_1 \\ P_2 \\ Q_2 \end{bmatrix} = B\begin{bmatrix} P^- \exp(-k\xi) \\ Q^- \exp(-k\xi) \\ Q^- kc \exp(-k\xi) \end{bmatrix} \tag{9}$$

where

$$B = \begin{bmatrix} E_1 & E_2 & E_1 \\ F_1 & F_2 & F_3 \\ G_1 & G_2 & G_3 \\ H_1 & H_2 & H_3 \end{bmatrix} \tag{10}$$

and values of E_1, E_2, F_1 $etc.$ are placed in Appendix 2.

By substituting values of L_1, M_1, P_1, Q_1 and L_2, M_2, P_2, Q_2 in the integral expressions for Airy stress function, stresses and displacements and on solving these integrals (Appendix 2), we get the results for Medium –I and II as follows:

$$U^{(I)} = L^-[E_1 \tan^{-1}(\tfrac{y}{\xi-z}) + F_1 z \ R_1] + M^-[E_2 \tan^{-1}(\tfrac{y}{\xi-z}) + F_2 z R_1 + E_1 \xi R_1 + 2F_3 \xi z R_1 R_2] +$$

$$P^-[-E_1 \ lnR + \ F_1 z R_2] + Q^-[-E_2 lnR + (F_2 z + E_1 \xi) \ R_2 + \ F_3 \xi z \tfrac{1}{R^2}\{2R_3 - 1\}] \tag{11}$$

$$\tau_{22}^{(I)} = L^-[2(E_1 + 2F_1)R_1R_2 + F_1z\frac{2R_1}{R^2}\{4R_3 - 1\}] + M^-[2(E_2 + 2F_2)R_1R_2 + (E_1\xi + 2F_3\xi +$$
$$F_2z)\frac{2R_1}{R^2}\{4R_3 - 1\} + 24F_3\xi zR_1R_4\{2R_3 - 1\}] + P^-[(E_1 + 2F_1)\frac{1}{R^2}\{2R_3 - 1\} +$$
$$2F_1z\,R_4\{4R_3 - 3\}] + \ Q^-[(E_2 + 2F_2)\frac{1}{R^2}\{2R_3 - 1\} + 2(E_1\xi + 2F_3\xi +$$
$$F_2z)R_4\{4R_3 - 3\} + F_3\xi z\frac{6}{R^4}\{8R_3^2 - 8R_3 + 1\}] \tag{12}$$

$$\tau_{23}^{(I)} = L^-[-(E_1 + F_1)\frac{1}{R^2}\{2R_3 - 1\} - 2F_1zR_4\{4R_3 - 3\}] + M^-[-(E_2 + F_2)\frac{1}{R^2}\{2R_3 - 1\} -$$
$$2(E_1\xi + F_3\xi + F_2z)R_4\{4R_3 - 3\} - F_3\xi z\frac{6}{R^4}\{8R_3^2 - 8R_3 + 1\}] + P^-[2(E_1 + F_1)R_1R_2 +$$
$$F_1z\frac{2R_1}{R^2}\{4R_3 - 1\}] + Q^-[2(E_2 + F_2)R_1R_2 + (E_1\xi + F_3\xi + F_2z)\frac{2R_1}{R^2}\{4R_3 - 1\} +$$
$$24F_3\xi zR_1R_4\{2R_3 - 1\}] \tag{13}$$

$$\tau_{33}^{(I)} = L^-[-2E_1R_1R_2 - F_1z\frac{2R_1}{R^2}\{4R_3 - 1\}] + M^-[-2E_2R_1R_2 - (E_1\xi + F_2z)\frac{2R_1}{R^2}\{4R_3 - 1\} -$$
$$24F_3\xi zR_1R_4\,\{2R_3 - 1\}] + P^-[-E_1\frac{1}{R^2}\{2R_3 - 1\} - 2F_1zR_4\{4R_3 - 3\}] + Q^-[-E_2\frac{1}{R^2}\{2R_3 -$$
$$1\} - 2(E_1\xi + \ F_2z)R_4\{4R_3 - 3\} - F_3\xi z\,\frac{6}{R^4}\{8R_3^2 - 8R_3 + 1\}] \tag{14}$$

$$2\mu_1u_2^{(I)} = L^-[-(E_1 + \frac{F_1}{\alpha_1})R_2 - F_1z\frac{1}{R^2}\{2R_3 - 1\}] + M^-[-(E_2 + \frac{F_2}{\alpha_1})R_2 - (E_1\xi + \frac{\xi F_3}{\alpha_1} + F_2z)\frac{1}{R^2}\{2R_3 -$$
$$1\} - 2\,F_3\xi zR_4\{4R_3 - 3\}] + P^-[(E_1 + \frac{F_1}{\alpha_1})R_1 + 2F_1zR_1R_2] + Q^-[(E_2 + \frac{F_2}{\alpha_1})R_1 + 2(E_1\xi +$$
$$\frac{\xi F_3}{\alpha_1} + \ F_2z)R_1R_2 + F_3\xi z\frac{2R_1}{R^2}\{4R_3 - 1\}] \tag{15}$$

$$2\mu_1u_3^{(I)} = L^-[-(E_1 + F_1 - \frac{F_1}{\alpha_1})R_1 - 2F_1zR_1R_2] + M^-[-(E_2 + F_2 - \frac{F_2}{\alpha_1})R_1 - 2(E_1\xi + F_3\xi - \frac{\xi F_3}{\alpha_1} +$$
$$F_2z)R_1R_2 - F_3\xi z\frac{2R_1}{R^2}\{4R_3 - 1\}] + P^-[-(E_1 + F_1 - \frac{F_1}{\alpha_1})R_2 - F_1z\frac{1}{R^2}\{2R_3 - 1\}] +$$
$$Q^-[-(E_2 + F_2 - \frac{F_2}{\alpha_1})R_2 - (E_1\xi + F_3\xi - \frac{\xi F_3}{\alpha_1} + F_2z)\frac{1}{R^2}\{2R_3 - 1\} - 2F_3\xi zR_4\{4R_3 - 3\}] \tag{16}$$

$$U^{(II)} = L_0\tan^{-1}(\frac{y}{|z-\xi|}) + M_0|z - \xi|R_1 - P_0\ln R + Q_0R_2 + L^-[G_1\tan^{-1}(\frac{y}{z+\xi}) + H_1zS_1] +$$
$$M^-[G_2\tan^{-1}(\frac{y}{z+\xi}) + (H_2z + G_3\xi)S_1 + 2H_3\xi zS_1S_2] + P^-[-G_1lnS + H_1S_2] +$$
$$Q^-[-G_2lnS + (H_2z + G_3\xi)S_2 + H_3\xi z\frac{1}{S^2}\{2S_3 - 1\}] \tag{17}$$

$$\tau_{22}^{(II)} = 2L_0|z - \xi|\frac{R_1}{R^2} + M_0\left[-4|z - \xi|\frac{R_1}{R^2} + |z - \xi|\frac{2R_1}{R^2}\{4R_3 - 1\}\right] + P_0\frac{1}{R^2}\{2R_3 - 1\} + Q_0[-2\frac{1}{R^2}\{2R_3 -$$
$$1\} + 2R_2^2\{4R_3 - 3\}] + L^-[2(G_1 - 2H_1)S_1S_2 + H_1z\frac{2S_1}{S^2}\{4S_3 - 1\}] + M^-[2(G_2 - 2H_2)S_1S_2 +$$
$$(G_3\xi - 2H_3\xi + H_2z)\frac{2S_1}{S^2}\{4S_3 - 1\} + 24H_3\xi zS_1S_4\{2S_3 - 1\}] + P^-[(G_1 - 2H_1)\frac{1}{S^2}\{2S_3 - 1\} +$$
$$2H_1zS_4\{4S_3 - 3\}] + \ Q^-[(G_2 - 2H_2)\frac{1}{S^2}\{2S_3 - 1\} + 2(G_3\xi - 2H_3\xi +$$
$$H_2z)S_4\{4S_3 - 3\} + H_3\xi z\frac{6}{S^4}\{8S_3^2 - 8S_3 + 1\}] \tag{18}$$

$$\tau_{23}^{(II)} = \pm[L_0\frac{1}{R^2}\{2R_3 - 1\} - M_0\frac{1}{R^2}\{2R_3 - 1\} + 2M_0R_2^2\{4R_3 - 3\} - P_02|z - \xi|\frac{y}{R^4} + Q_02|z - \xi|\frac{y}{R^4} -$$
$$Q_0|z - \xi|\frac{2y}{R^4}\{4R_3 - 1\}] + L^-[(G_1 - H_1)\frac{1}{S^2}\{2S_3 - 1\} + 2H_1zS_4\{4S_3 - 3\}] + M^-[(G_2 -$$
$$H_2)\frac{1}{S^2}\{2S_3 - 1\} + 2(G_3\xi - H_3\xi + H_2z)\,S_4\{4S_3 - 3\} + \ H_3\xi z\frac{6}{S^4}\{8S_3^2 - 8S_3 + 1\}] +$$
$$P^-[-2(G_1 - H_1)S_1S_2 - H_1z\frac{2y}{S^4}\{4S_3 - 1\}] + Q^-[-2(G_2 - H_2)S_1S_2 - (G_3\xi - H_3\xi +$$
$$H_2z)\frac{2y}{S^4}\{4S_3 - 1\} - 24H_3\xi zS_1S_4\{2S_3 - 1\}] \tag{19}$$

$$\tau_{33}^{(II)} = -L_02|z - \xi|\frac{y}{R^4} - M_0|z - \xi|\frac{2y}{R^4}\{4R_3 - 1\} - P_0\frac{1}{R^2}\{2R_3 - 1\} - 2Q_0R_2^2\{4R_3 - 3\} +$$
$$L^-\left[-2G_1S_1S_2 - H_1z\frac{2y}{S^4}\{4S_3 - 1\}\right] + M^-[-2G_2S_1S_2 - (G_3\xi + H_2z)\frac{2y}{S^4}\{4S_3 - 1\} -$$
$$24H_3\xi zS_1S_4\{2S_3 - 1\}] + P^-[-G_1\frac{1}{S^2}\{2S_3 - 1\} - 2H_1zS_4\{4S_3 - 3\}] +$$
$$Q^-[-G_2\frac{1}{S^2}\{2S_3 - 1\} - 2(G_3\xi + H_2z)S_4\{4S_3 - 3\} - H_3\xi z\frac{6}{S^4}\{8S_3^2 - 8S_3 + 1\}] \tag{20}$$

$$2\mu_2 u_2^{(II)} = -L_0 \frac{|z-\xi|}{R^2} + \frac{M_0}{\alpha_2}\frac{|z-\xi|}{R^2} - M_0|z-\xi|\frac{1}{R^2}\{2R_3 - 1\} + P_0 R_1 - \frac{Q_0}{\alpha_2}R_1 + 2Q_0(z-\xi)^2 \frac{R_1}{R^2} +$$
$$L^-[(-G_1 + H_1/\alpha_2)S_2 - H_1 z \frac{1}{S^2}\{2S_3 - 1\}] + M^-[(-G_2 + H_2/\alpha_2)S_2 + (-G_3\xi +$$
$$\frac{\xi H_3}{\alpha_2} - H_2 z)\frac{1}{S^2}\{2S_3 - 1\} - 2H_3\xi z S_4\{4S_3 - 3\}] + P^-[(G_1 - H_1/\alpha_2)S_1 + 2H_1 z S_1 S_2] +$$
$$Q^-[(G_2 - H_2/\alpha_2)S_1 + 2(G_3\xi - \xi H_3/\alpha_2 + H_2 z)S_1 S_2 + H_3\xi z \frac{2y}{S^4}\{4S_3 - 1\}] \qquad (21)$$

$$2\mu_2 u_3^{(II)} = \pm\left[(L_0 - M_0 + \frac{M_0}{\alpha_2})R_1 + 2M_0(z-\xi)^2 \frac{y}{R^4} + (P_0 - Q_0 + \frac{Q_0}{\alpha_2})\frac{|z-\xi|}{R^2} + Q_0|z - \right.$$
$$\left.\xi|\frac{1}{R^2}\{2R_3 - 1\}\right] + L^-[(G_1 - H_1 + H_1/\alpha_2)S_1 + 2H_1 z S_1 S_2] + M^-[(G_2 - H_2 +$$
$$H_2/\alpha_2)S_1 + 2(G_3\xi - \xi H_3 + \frac{\xi H_3}{\alpha_2} + H_2 z)S_1 S_2 + H_3\xi z \frac{2y}{S^4}\{4S_3 - 1\}] + P^-[(G_1 -$$
$$H_1 + H_1/\alpha_2)S_2 + H_1 z \frac{1}{S^2}\{2S_3 - 1\}] + Q^-[(G_2 - H_2 + H_2/\alpha_2)S_2 +$$
$$(G_3\xi - \xi H_3 + \frac{\xi H_3}{\alpha_2} + H_2 z)\frac{1}{S^2}\{2S_3 - 1\} + 2H_3\xi z S_4\{4S_3 - 3\}] \qquad (22)$$

where
$$R^2 = y^2 + (z-\xi)^2,$$
$$S^2 = y^2 + (z+\xi)^2,$$
$$R_1 = \frac{y}{R^2}; R_2 = \frac{\xi-z}{R^2}; R_3 = \frac{(\xi-z)^2}{R^2}; R_4 = \frac{\xi-z}{R^4}; S_1 = \frac{y}{S^2}; S_2 = \frac{\xi+z}{S^2}; S_3 = \frac{(\xi+z)^2}{S^2}; S_4 = \frac{\xi+z}{S^4}.$$

1 Perfect Interface Case

If we substitute $k_{22}=k_{33}=1$ in equations (11) to (22), we get the analytic form for displacements and stresses for two perfectly joined half-spaces, which coincides with the results of Singh et al. [3].

2 Traction-Free Interface Case

If we substitute $k_{22}=k_{33}=0$ in equations (11) to (22), we get the analytic form for displacements and stresses for two joined half-spaces having traction-free interface or sliding interface.

DISPLACEMENTS AND STRESSES FOR VERTICAL DIP-SLIP AND TENSILE FAULTS

In this section, we have obtained displacements and stresses due to vertical dip-slip and tensile faults.

1 Vertical Dip-Slip Fault

Fault is defined as a plane fracture between two blocks and dip is defined as angle of the fault with respect to the surface. Vertical dip-slip fault occurred due to double couple (23) + (32) mechanism of seismic sources which allow relative movement of blocks vertically [Figure 2], and moment of double couple D_{23} is given by Singh et al. [3] as follows,

$$D_{23} = \mu_2 bds$$
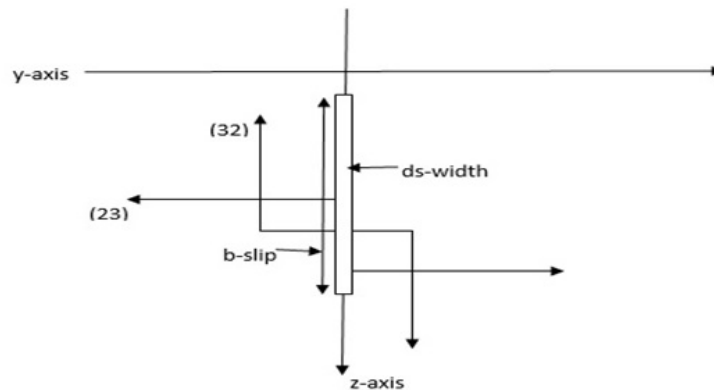
where μ_2 is the rigidity of medium II.

Fig. 2 Geometry of double couple mechanism of source resulting vertical dip-slip fault

By substituting the values of source coefficients from Table 1 in (11) to (22), we get displacements and stresses generated by vertical dip-slip fault,

$$U^{(I)} = -\frac{\alpha_2 \mu_2 bds}{\pi} [E_2 \tan^{-1}(\frac{y}{\xi-z}) + F_2 z R_1 + E_1 \xi R_1 + 2F_3 \xi z R_1 R_2] \tag{23}$$

$$\tau_{22}^{(I)} = -\frac{\alpha_2 \mu_2 bds}{\pi} [\, 2(E_2 + 2F_2) R_1 R_2 + (E_1 \xi + 2F_3 \xi + F_2 z) \frac{2y}{R^4}\{4R_3 - 1\} + 24F_3 \xi z R_1 R_4\{2R_3 - 1\}] \tag{24}$$

$$\tau_{23}^{(I)} = -\frac{\alpha_2 \mu_2 bds}{\pi} [-(E_2 + F_2) \frac{1}{R^2}\{2R_3 - 1\} - 2(E_1 \xi + F_3 \xi + F_2 z) R_4\{4R_3 - 3\} - F_3 \xi z \frac{6}{R^4}\{8R_3^2 - 8R_3 + 1\}] \tag{25}$$

$$\tau_{33}^{(I)} = -\frac{\alpha_2 \mu_2 bds}{\pi} [-2E_2 R_1 R_2 - (E_1 \xi + F_2 z) \frac{2y}{R^4}\{4R_3 - 1\} - 24F_3 \xi z \, R_1 R_4\{2R_3 - 1\}] \tag{26}$$

$$2\mu_1 u_2^{(I)} = -\frac{\alpha_2 \mu_2 bds}{\pi} [-(E_2 + \frac{F_2}{\alpha_1}) R_2 - (E_1 \xi + \frac{\xi F_3}{\alpha_1} + F_2 z) \frac{1}{R^2}\{2R_3 - 1\} - 2\, F_3 \xi z R_4\{4R_3 - 3\} \tag{27}$$

$$2\mu_1 u_3^{(I)} = -\frac{\alpha_2 \mu_2 bds}{\pi} [-(E_2 + F_2 - \frac{F_2}{\alpha_1}) R_1 - 2(E_1 \xi + F_3 \xi - \frac{\xi F_3}{\alpha_1} + F_2 z) R_1 R_2 - F_3 \xi z \frac{2y}{R^4}\{4R_3 - 1\}] \tag{28}$$

$$U^{(II)} = \frac{\alpha_2 \mu_2 bds}{\pi} \left[(z - \xi) R_1 - G_2 \tan^{-1}(\frac{y}{z+\xi}) - (H_2 z + G_3 \xi) S_1 - 2H_3 \xi z S_1 S_2 \right] \tag{29}$$

$$\tau_{22}^{(II)} = \frac{\alpha_2 \mu_2 bds}{\pi} [4R_1 R_2 - 2R_1 R_2\{4R_3 - 1\} - 2(G_2 - 2H_2) S_1 S_2 - (G_3 \xi - 2H_3 \xi + H_2 z) \frac{2y}{S^4}\{4S_3 - 1\} - 24H_3 \xi z S_1 S_4\{2S_3 - 1\}] \tag{30}$$

$$\tau_{23}^{(II)} = \frac{\alpha_2 \mu_2 bds}{\pi} [-\frac{1}{R^2}\{2R_3 - 1\} + 2R_2^2\{4R_3 - 3\} - (G_2 - H_2) \frac{1}{S^2}\{2S_3 - 1\} - 2(G_3 \xi - H_3 \xi + H_2 z) S_4\{4S_3 - 3\} - H_3 \xi z \frac{6}{S^4}\{8S_3^2 - 8S_3 + 1\}] \tag{31}$$

$$\tau_{33}^{(II)} = -\frac{\alpha_2 \mu_2 bds}{\pi} \left[(z - \xi) \frac{2y}{R^4}\{4R_3 - 1\} + 2G_2 S_1 S_2 + (G_3 \xi + H_2 z) \frac{2y}{S^4}\{4S_3 - 1\} + 24H_3 \xi z S_1 S_4\{2S_3 - 1\} \right] \tag{32}$$

$$2\mu_2 u_2^{(II)} = \frac{\alpha_2 \mu_2 bds}{\pi} \left[-\frac{R_2}{\alpha_2} + R_2\{2R_3 - 1\} \right] - (-G_2 + \frac{H_2}{\alpha_2}) S_2 - (-G_3 \xi + \frac{\xi H_3}{\alpha_2} - H_2 z) \frac{1}{S^2}\{2S_3 - 1\} + 2H_3 c z S_4\{4S_3 - 3\}] \tag{33}$$

$$2\mu_2 u_3^{(II)} = \frac{\alpha_2 \mu_2 bds}{\pi} [-R_1 + \frac{1}{\alpha_2} R_1 + 2R_1 R_3 - (G_2 - H_2 + H_2/\alpha_2) S_1 - 2(G_3 \xi - \xi H_3 + \frac{\xi H_3}{\alpha_2} + H_2 z) S_1 S_2 - H_3 \xi z \frac{2y}{S^4}\{4S_3 - 1\}] \tag{34}$$

2   Tensile fault

We have considered two tensile faults vertical and horizontal, defined as a vertical tensile fault occurred due to dipole (22) mechanism of seismic source with dislocation in the y-direction.

A horizontal tensile fault occurred due to dipole (33) mechanism of seismic source with dislocation in the z-direction.

Analytic expressions for displacements and stresses due to tensile fault by substituting corresponding values of seismic source coefficients from Table 1 and $T_0 = \mu_2 bds$ (S.J. Singh & Singh [6]), are obtained as follows;

$$U^{(I)} = \frac{\alpha_2 \mu_2 bds}{\pi} [\, -E_1 \ln R + \ F_1 z R_2 \pm E_2 \ln R \mp (F_2 z + E_1 \xi) R_2 \mp F_3 \xi z \frac{1}{R^2}\{2R_3 - 1\}] \tag{35}$$

$$\tau_{22}^{(I)} = \frac{\alpha_2 \mu_2 bds}{\pi} [(E_1 + 2F_1) \frac{1}{R^2}\{2R_3 - 1\} + 2\, F_1 z R_4 \{4R_3 - 3\} \mp (E_2 + 2F_2) \frac{1}{R^2}\{2R_3 - 1\} \mp 2(E_1 \xi + 2F_3 \xi + F_2 z) R_4\{4R_3 - 3\} \mp F_3 \xi z \frac{6}{R^4}\{8R_3^2 - 8R_3 + 1\}] \tag{36}$$

$$\tau_{23}^{(I)} = \frac{\alpha_2 \mu_2 bds}{\pi} [2(E_1 + F_1) R_1 R_2 + F_1 z \frac{2y}{R^4}\{4R_3 - 1\} \mp 2(E_2 + F_2) R_1 R_2 \mp (E_1 \xi + F_3 \xi + F_2 z) \frac{2y}{R^4}\{4R_3 - 1\} \mp 24F_3 \xi z R_1 R_4\{2R_3 - 1\}] \tag{37}$$

$$\tau_{33}^{(I)} = \frac{\alpha_2 \mu_2 bds}{\pi}\left[-E_1\frac{1}{R^2}\{2R_3-1\}-2F_1zR_4\{4R_3-3\}\pm E_2\frac{1}{R^2}\{2R_3-1\}\pm 2(E_1\xi+ \right.$$
$$\left. F_2z\Big)R_4\{4R_3-3\}\pm F_3\xi z\frac{6}{R^4}\{8R_3^2-8R_3+1\}\right] \tag{38}$$

$$2\mu_1 u_2^{(I)} = \frac{\alpha_2 \mu_2 bds}{\pi}\left[(E_1+\frac{F_1}{\alpha_1})R_1+2F_1zR_1R_2\mp(E_2+\frac{F_2}{\alpha_1})R_1\mp 2(E_1\xi+\frac{\xi F_3}{\alpha_1}+ \right.$$
$$\left. F_2z)R_1R_2\mp F_3\xi z\frac{2y}{R^4}\{4R_3-1\}\right] \tag{39}$$

$$2\mu_1 u_3^{(I)} = \frac{\alpha_2 \mu_2 bds}{\pi}\left[-(E_1+F_1-\frac{F_1}{\alpha_1})R_2-F_1z\frac{1}{R^2}\{2R_3-1\}\pm(E_2+F_2-\frac{F_2}{\alpha_1})R_2\pm \right.$$
$$\left. (E_1\xi+F_3\xi-\frac{\xi F_3}{\alpha_1}+F_2z)\frac{1}{R^2}\{2R_3-1\}\pm 2F_3\xi zR_4\{4R_3-3\}\right] \tag{40}$$

$$U^{(II)} = \frac{\alpha_2 \mu_2 bds}{\pi}\left[-\ln R\mp R_3-G_1 lnS+H_1zS_2\pm G_2 lnS\mp(H_2z+G_3\xi)S_2\mp H_3\xi z\frac{1}{S^2}\{2S_3-1\}\right] \tag{41}$$

$$\tau_{22}^{(II)} = \frac{\alpha_2 \mu_2 bds}{\pi}\left[\frac{1}{R^2}\{2R_3-1\}\pm 2\frac{1}{R^2}\{2R_3-1\}\mp 2R_2^2\{4R_3-3\}+(G_1-2H_1)\frac{1}{S^2}\{2S_3-1\}+ \right.$$
$$2H_1zS_4\{4S_3-3\}\mp(G_2-2H_2)\frac{1}{S^2}\{2S_3-1\}\mp 2(G_3\xi-2H_3\xi+H_2z)S_4\{4S_3-3\}\mp$$
$$\left. H_3\xi z\frac{6}{S^4}\{8S_3^2-8S_3+1\}\right] \tag{42}$$

$$\tau_{23}^{(II)} = \frac{\alpha_2 \mu_2 bds}{\pi}\left[2R_1R_2\pm 2R_1R_2\mp 2R_1R_2\{4R_3-1\}-2(G_1-H_1)S_1S_2-H_1z\frac{2y}{S^4}\{4S_3-1\}\pm \right.$$
$$\left. 2(G_2-H_2)S_1S_2\pm(G_3\xi-H_3\xi+H_2z)\frac{2y}{S^4}\{4S_3-1\}\pm 24H_3\xi zS_1S_4\{2S_3-1\}\right] \tag{43}$$

$$\tau_{33}^{(II)} = \frac{\alpha_2 \mu_2 bds}{\pi}\left[-\frac{1}{R^2}\{2R_3-1\}\pm 2R_2^2\{4R_3-3\}-G_1\frac{1}{S^2}\{2S_3-1\}-2H_1zS_4\{4S_3-3\}\pm \right.$$
$$\left. G_2\frac{1}{S^2}\{2S_3-1\}\pm 2(G_3\xi+H_2z\Big)S_4\{4S_3-3\}\pm H_3\xi z\frac{6}{S^4}\{8S_3^2-8S_3+1\}\right] \tag{44}$$

$$2\mu_2 u_2^{(II)} = \frac{\alpha_2 \mu_2 bds}{\pi}\left[R_1(1\pm\frac{1}{\alpha_2}\mp 2R_3)+(G_1-H_1/\alpha_2)S_1+2H_1zS_1S_2\mp(G_2-H_2/\alpha_2)S_1\mp \right.$$
$$\left. 2(G_3\xi-\xi H_3/\alpha_2+H_2z)S_1S_2\mp H_3\xi z\frac{2y}{S^4}\{4S_3-1\}\right] \tag{45}$$

$$2\mu_2 u_3^{(II)} = \frac{\alpha_2 \mu_2 bds}{\pi}\left[-R_2\{1\pm 1\mp\frac{1}{\alpha_2}\}\pm R_2\left\{\frac{2(z-\xi)^2}{R^2}-1\right\}+(G_1-H_1+H_1/\alpha_2)S_2+ \right.$$
$$H_1z\frac{1}{S^2}\{2S_3-1\}\mp(G_2-H_2+H_2/\alpha_2)S_2\mp(G_3\xi-\xi H_3+\frac{\xi H_3}{\alpha_2}+$$
$$\left. H_2z)\frac{1}{S^2}\{2S_3-1\}\mp 2H_3\xi zS_4\{4S_3-3\}\right] \tag{46}$$

where upper sign stands for vertical tensile fault and lower sign for horizontal tensile fault.

NUMERICAL DISCUSSIONS WITH GRAPHS AND MESH GRIDS

In this section, we have numerically discussed the results with the help of graphs and mesh grids. we have applied dimensionless approach to study the effects of force like imperfect interface on transmission of stresses across the interface, For numerical calculations, we have taken continental crust model, *i.e.* $\alpha_1 = \alpha_2 = 0.685 \ \& \ \beta = 0.451$. For plotting graphs, consider dimensionless quantities $Y = \frac{y}{\xi}$ *(Distance from the fault) and* $Z = \frac{z}{\xi}$ *(Distance from the interface)*, where ξ is the distance of the line source from the interface. The displacements and stresses are measured in units of $\frac{bds}{\pi\xi}$ *and* $\frac{\mu_2 bds}{\pi\xi^2}$ respectively. Let the dimensionless displacements and stresses be denoted by $U_i^{(I)}, U_i^{(II)}, \sigma_{ij}^{(I)} \& \sigma_{ij}^{(II)}$; then

$$U_i^{(I)} = \frac{\pi\xi u_i^{(I)}}{bds} \ and \ U_i^{(II)} = \frac{\pi\xi u_i^{(II)}}{bds}; \ \sigma_{ij}^{(I)} = \frac{\pi\xi^2 \tau_{ij}^{(I)}}{\mu_2 bds} \ and \ \sigma_{ij}^{(II)} = \frac{\pi\xi^2 \tau_{ij}^{(II)}}{\mu_2 bds}$$

Figures 3 to 8 are depicting variations in Dimensionless normal and shear stresses for different bonding conditions caused by vertical dip-slip fault in Medium-I & II with distance from the fault. It is observed that stresses are greater in magnitude for perfect bonding conditions as compare to imperfect bonding conditions in Medium-I; however, in medium-II stresses behaved in opposite i.e. stresses are less in magnitude for perfect bonding conditions as compare to imperfect bonding conditions in Medium-II. Also there is significant variations in magnitude of stresses for corresponding different bonding conditions in

Medium-I as compare to medium-II. Normal stresses are antipodal symmetric and shear stresses are symmetric about Z-axis.
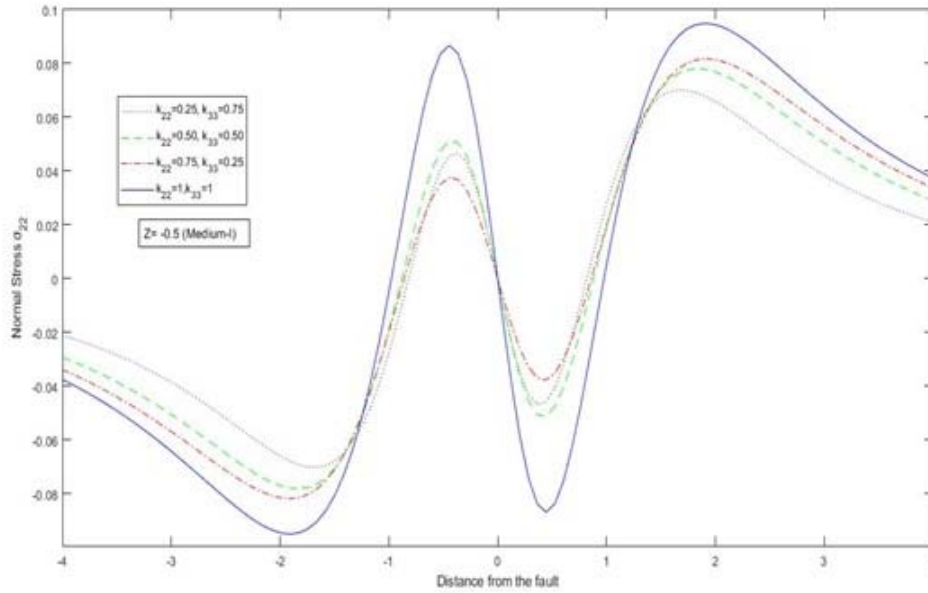

Fig. 3 Variations in Dimensionless normal stress σ_{22} for different bonding conditions due to vertical dip-slip fault in Medium-I
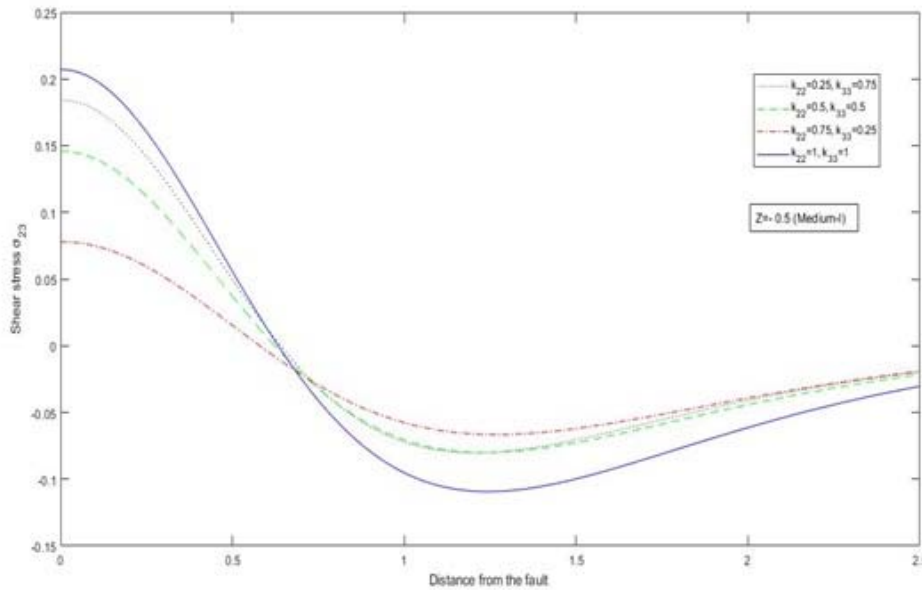

Fig. 4 Variations in Dimensionless shear stress σ_{23} for different bonding conditions due to vertical dip-slip fault in Medium-I
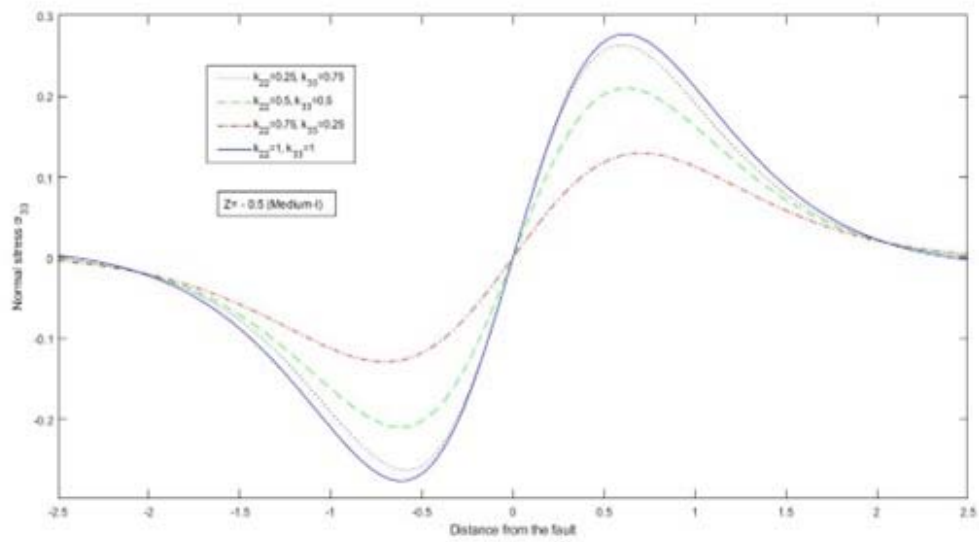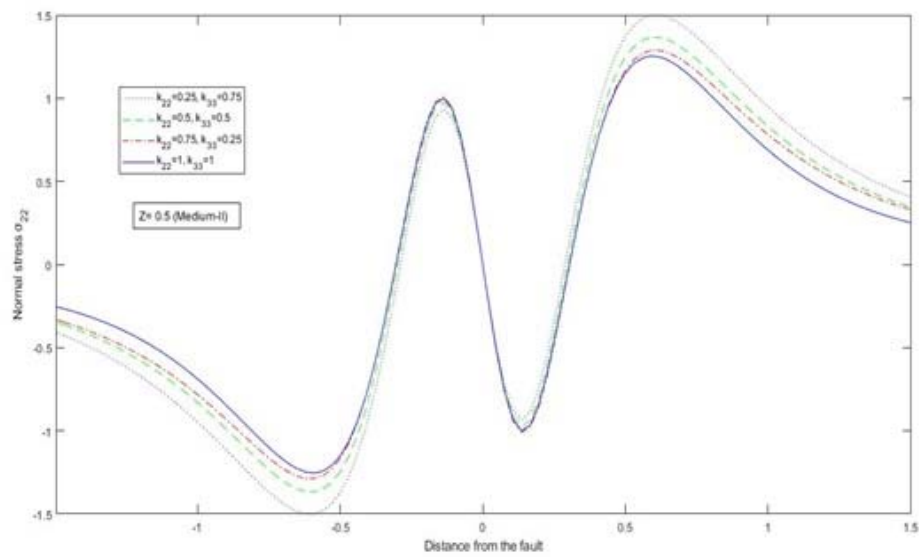
Fig. 5 Variations in Dimensionless normal stress σ_{33} for different bonding conditions due to vertical dip-slip fault in Medium-I

Fig. 6 Variations in Dimensionless normal stress σ_{22} for different bonding conditions due to vertical dip-slip fault in Medium-II
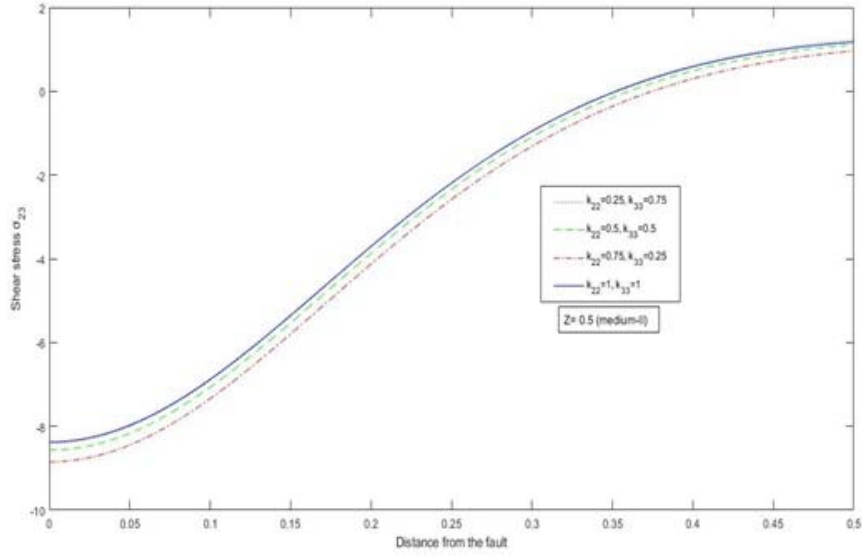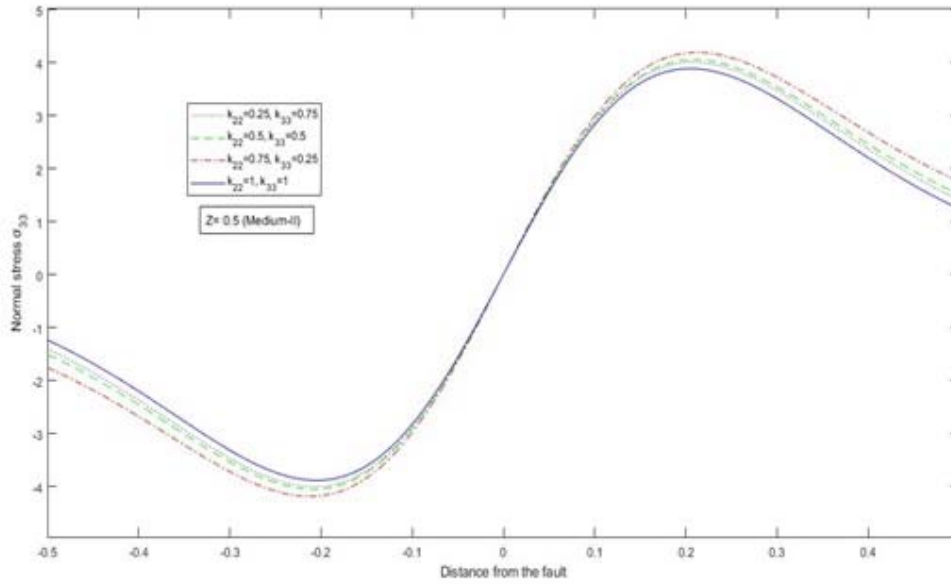
Fig. 7 Variations in Dimensionless shear stress σ_{23} for different bonding conditions due to vertical dip-slip fault in Medium-II

Fig. 8 Variations in Dimensionless normal stress σ_{33} for different bonding conditions due to vertical dip-slip fault in Medium-II

Figures 9 to 11 mesh grid maps are showing discontinuity in dimensionless normal and shear stresses at interface caused by vertical dip-slip fault.
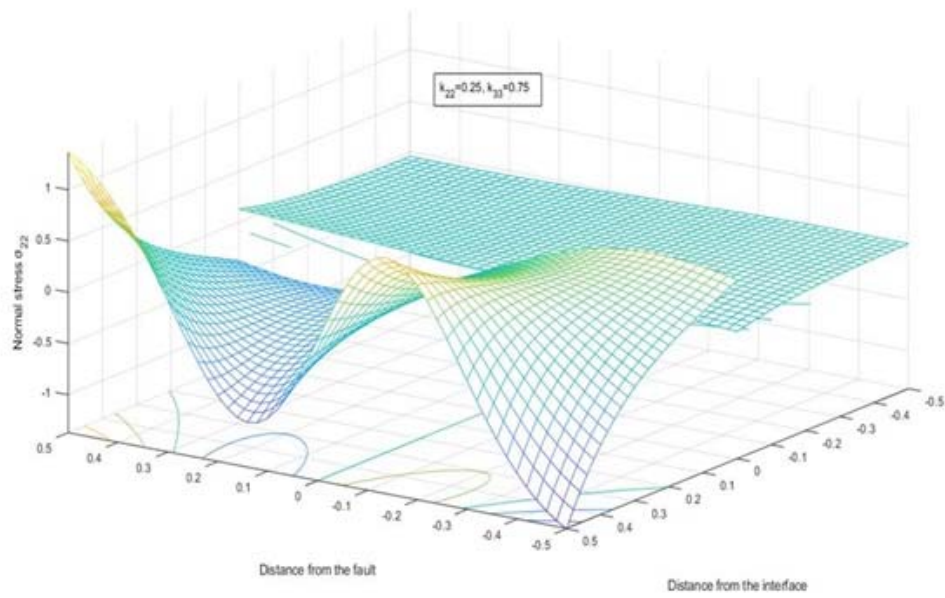
Fig. 9 Mesh grid Map showing discontinuity in dimensionless normal stress σ_{22} at interface generated by vertical dip-slip fault
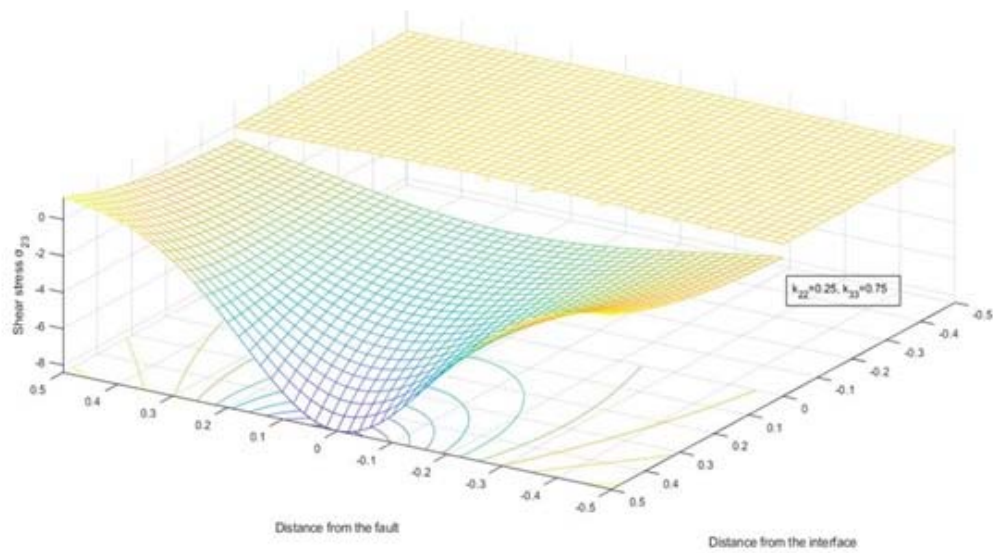

Fig. 10   Mesh grid Map showing discontinuity in dimensionless shear stress σ_{23} at interface generated by vertical dip-slip fault
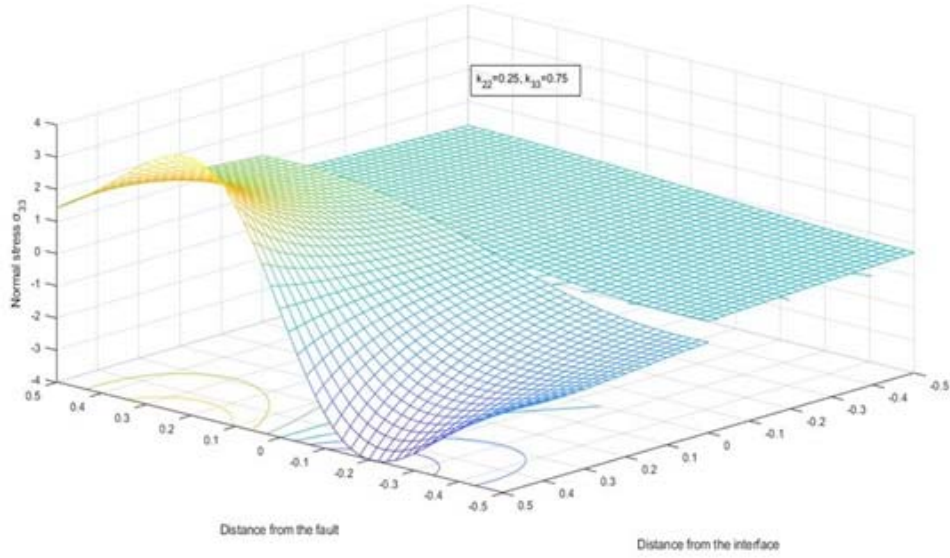
Fig. 11   Mesh grid Map showing discontinuity in dimensionless normal stress σ_{33} at interface
          generated by vertical dip-slip fault

Figures 12 to 16 mesh grid map showing the significant range of dimensionless stresses and
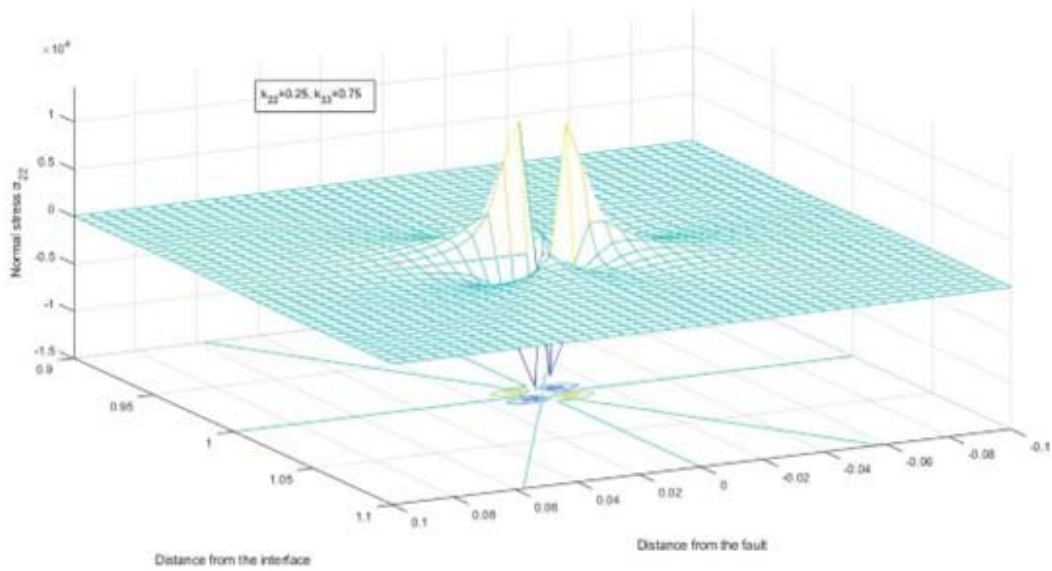displacements near the source caused by vertical dip-slip fault.

Fig. 12   Mesh grid Map depicting significant range of dimensionless normal stress σ_{22} generated
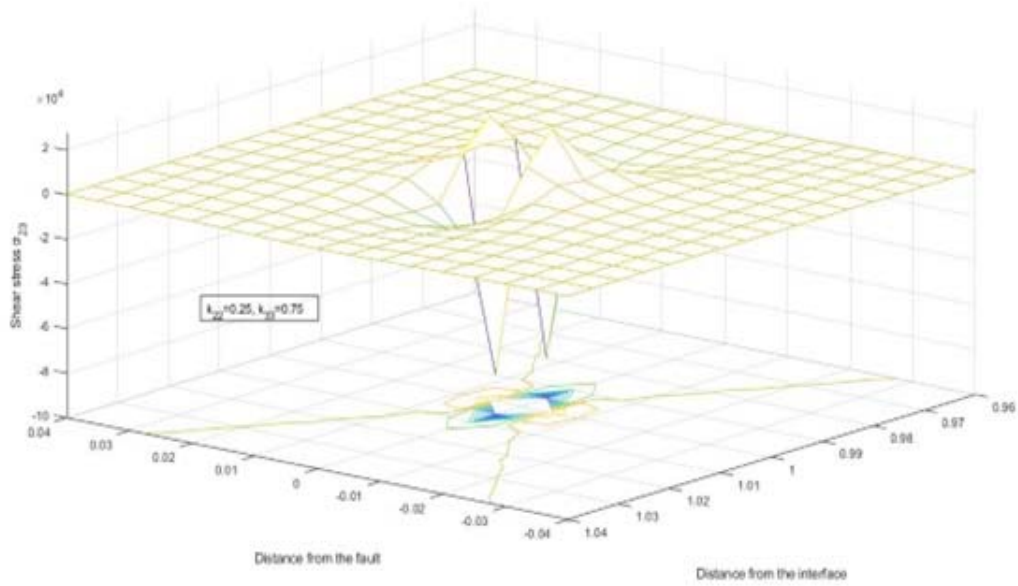   by vertical dip-slip fault

Fig. 13   Mesh grid Map depicting significant range of dimensionless shear stress σ_{23} generated by vertical dip-slip fault
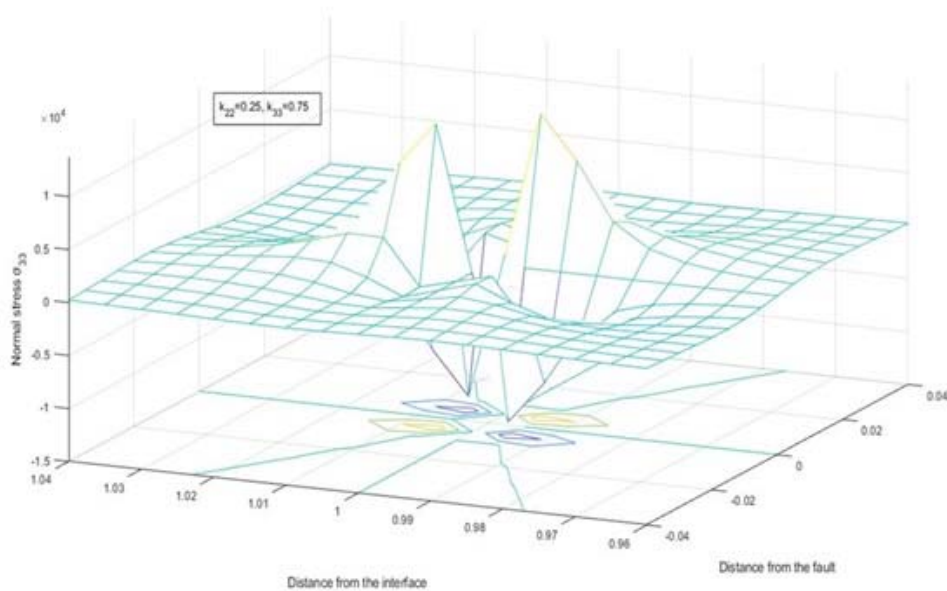

Fig. 14   Mesh grid Map depicting significant range of dimensionless normal stress σ_{33} generated by vertical dip-slip fault

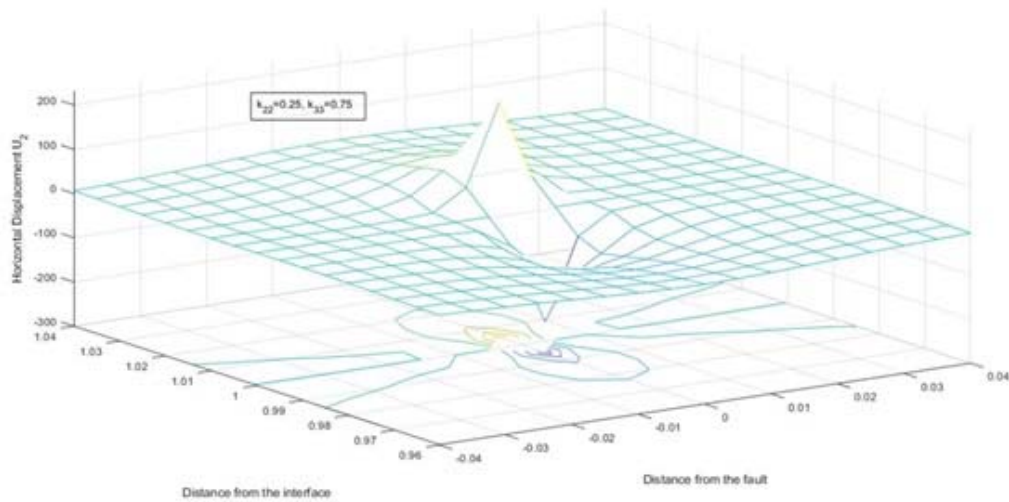Fig. 15   Mesh grid Map depicting significant range of dimensionless horizontal displacement U_2
generated by vertical dip-slip fault
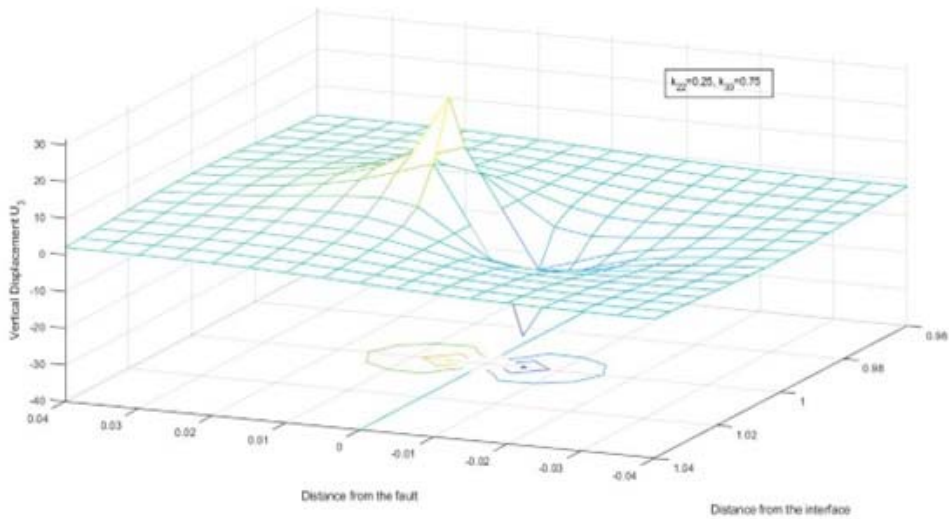
Fig. 16   Mesh grid Map depicting significant range of dimensionless vertical displacement U_3
generated by vertical dip-slip fault

Figures 17 to 19 mesh grid map showing discontinuity in dimensionless normal and shear stresses at
interface caused by horizontal tensile fault.

Fig. 17   Mesh grid Map showing discontinuity in dimensionless normal stress σ_{22} at interface generated by horizontal tensile fault

Fig. 18   Mesh grid Map showing discontinuity in dimensionless shear stress σ_{23} at interface generated by horizontal tensile fault

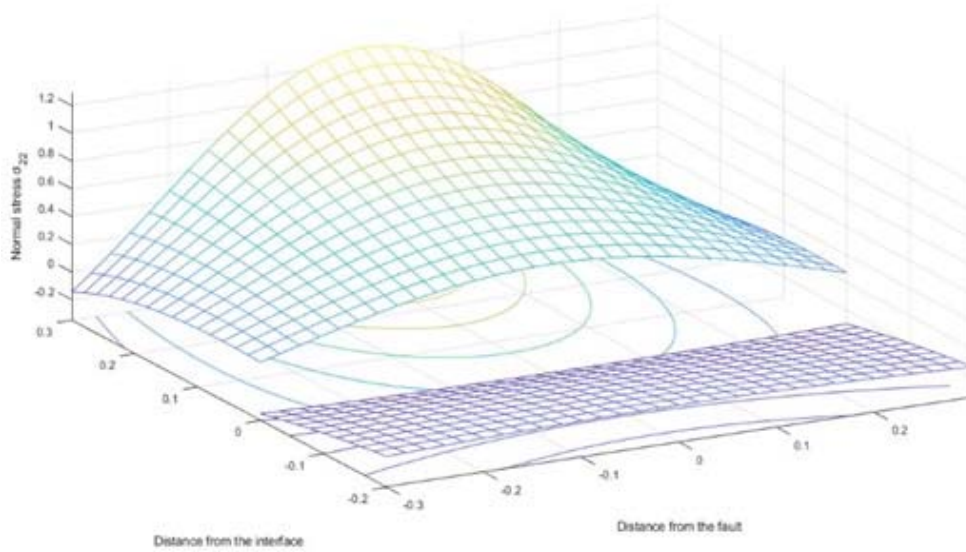Fig. 19   Mesh grid Map showing discontinuity in dimensionless normal stress σ_{33} at interface
           generated by horizontal tensile fault

   Figures 20 to 22 mesh grid map showing discontinuity in dimensionless normal and shear stresses at
interface caused by vertical tensile fault.
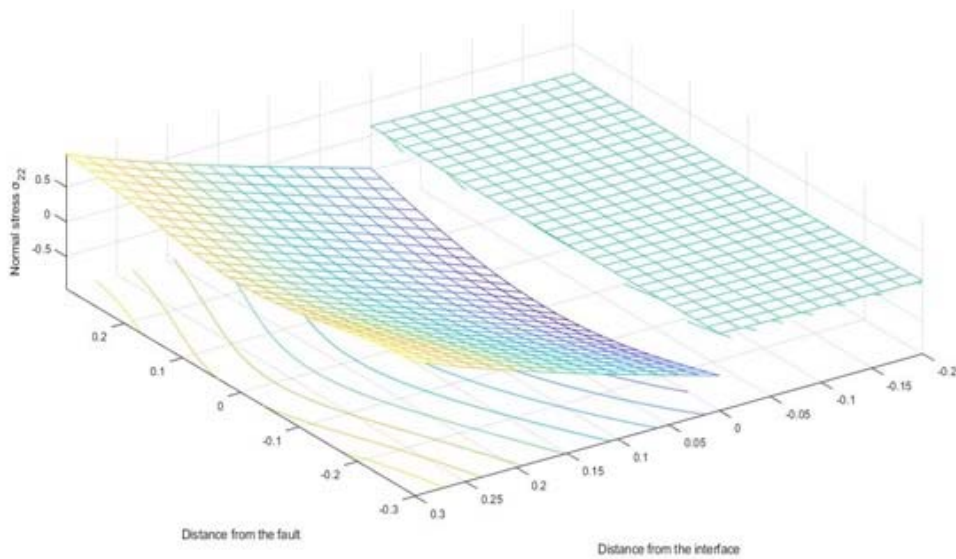
Fig. 20   Mesh grid Map showing discontinuity in dimensionless normal stress σ_{22} at interface
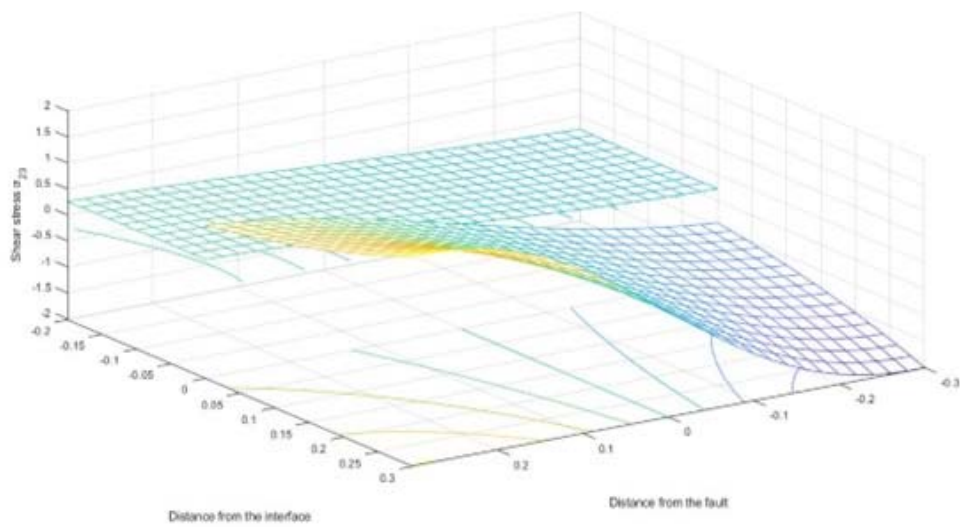   generated by vertical tensile fault
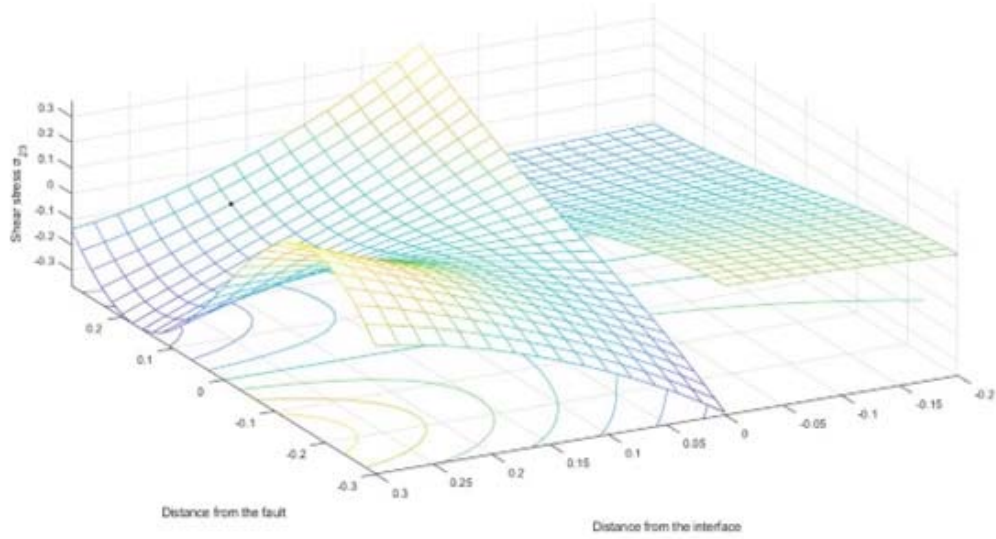
Fig. 21 Mesh grid Map showing discontinuity in dimensionless shear stress σ_{23} at interface generated by vertical tensile fault
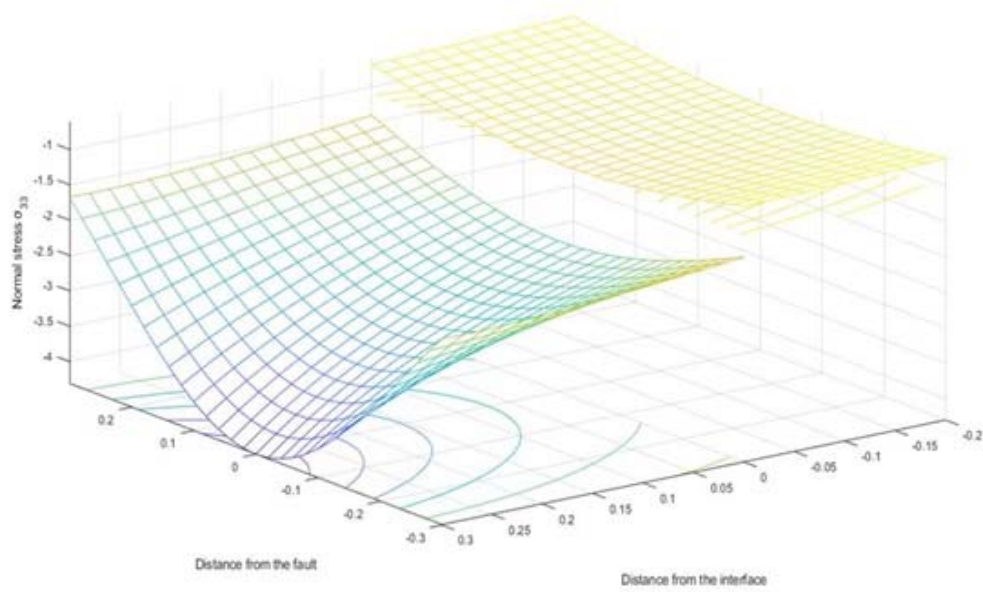

Fig. 22 Mesh grid Map showing discontinuity in dimensionless normal stress σ_{33} at interface generated by vertical tensile fault

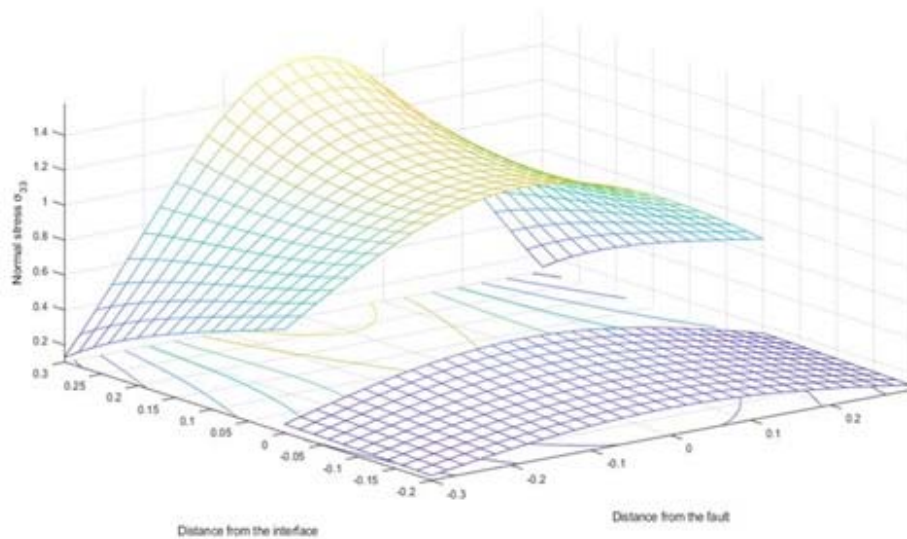From Figures 9 to 11 and 17 to 22, numerical results on jump discontinuity at interface are observed for different interface conditions for vertical dip-slip fault, horizontal tensile fault and vertical tensile fault. Magnitude of jump discontinuity are produced here in tabular form-

Magnitude of jump discontinuity at interface at a numerical glance:

Stress	Magnitude of jump disc.	Bonding conditions	Observations	Fault
σ_{22}	0.5044	$k_{22}=0.25$, $k_{33}=0.75$	Jump at interface is greater in magnitude for $k_{22}=0.75$, $k_{33}=0.25$ and less in magnitude for $k_{22}=0.25$, $k_{33}=0.75$; Significantly difference is observed in σ_{33} for different bonding conditions.	Vertical dip-slip
	0.7782	$k_{22}=0.5$, $k_{33}=0.5$		
	0.7417	$k_{22}=0.75$, $k_{33}=0.25$		
σ_{23}	0.7274	$k_{22}=0.25$, $k_{33}=0.75$		
	0.8061	$k_{22}=0.5$, $k_{33}=0.5$		
	0.9433	$k_{22}=0.75$, $k_{33}=0.25$		
σ_{33}	0.6618	$k_{22}=0.25$, $k_{33}=0.75$		
	1.0634	$k_{22}=0.5$, $k_{33}=0.5$		
	1.7507	$k_{22}=0.75$, $k_{33}=0.25$		
σ_{22}	0.0265	$k_{22}=0.25$, $k_{33}=0.75$	Significantly difference is observed in σ_{23} for different bonding conditions. Less effect of bonding conditions on transmission of stress σ_{22} across interface.	Horizontal tensile fault
	0.0251	$k_{22}=0.5$, $k_{33}=0.5$		
	0.1248	$k_{22}=0.75$, $k_{33}=0.25$		
σ_{23}	0.7003	$k_{22}=0.25$, $k_{33}=0.75$		
	0.189	$k_{22}=0.5$, $k_{33}=0.5$		
	0.1009	$k_{22}=0.75$, $k_{33}=0.25$		
σ_{33}	0.3139	$k_{22}=0.25$, $k_{33}=0.75$		
	0.5985	$k_{22}=0.5$, $k_{33}=0.5$		
	1.0396	$k_{22}=0.75$, $k_{33}=0.25$		
σ_{22}	0.0871	$k_{22}=0.25$, $k_{33}=0.75$	Jump at interface is greater in magnitude for $k_{22}=0.75$, $k_{33}=0.25$ and less in magnitude for $k_{22}=0.25$, $k_{33}=0.75$; Significantly difference is observed in σ_{23} for different bonding conditions.	Vertical tensile fault
	0.1825	$k_{22}=0.5$, $k_{33}=0.5$		
	0.3594	$k_{22}=0.75$, $k_{33}=0.25$		
σ_{23}	0.7604	$k_{22}=0.25$, $k_{33}=0.75$		
	1.1541	$k_{22}=0.5$, $k_{33}=0.5$		
	1.5306	$k_{22}=0.75$, $k_{33}=0.25$		
σ_{33}	0.202	$k_{22}=0.25$, $k_{33}=0.75$		
	0.2661	$k_{22}=0.5$, $k_{33}=0.5$		
	0.3728	$k_{22}=0.75$, $k_{33}=0.25$		

DISCUSSION

The two-phase model is considered in this research, which is useful for studying the consequences of internal structural discontinuities in the earth while neglecting the free surface. As earth is made up of many layers, and these layers are not perfectly joined, there are different kinds of imperfection at interfaces. Imperfect interface provides better information of transmission of stresses, displacements and strains from one medium to another medium rather than perfect. Outcomes of effects of imperfection at interface of two mediums is of great significance in the research of static deformation calculations caused by seismic sources. In real situations interfaces are rarely perfect, so for results due to imperfect interface conditions are more appropriate. Here, the mathematical representation of the displacements and stresses for two imperfectly joined half-spaces having force-like interface bonding generated by a line source is obtained. As in force-like interfaces, displacements are continuous across the interface but stresses are not, the work given in this research represents an advancement on prior findings on perfect and   traction-free interfaces. Stresses through force-like interface transmit less in magnitude. Strain energy will convey less in magnitude because strains are directly proportional to stresses. The results obtained here motivate to study, all possible interfaces lie between the perfect and traction-free interfaces. These findings can be used to create multiple frameworks for characterizing such applications.

CONCLUSION

We have obtained expressions for displacements and stresses generated by a line source for two elastic half-spaces having force-like imperfect bonding conditions at interface are obtained. Particular cases of vertical dip-slip and tensile faults are discussed numerically and graphically. Variations in normal and shear stresses by taking perfect and imperfect bonding conditions are perceived. By considering imperfection at

interface, a jump discontinuity in stresses is observed at interface. In medium-I, stresses are considerably lesser in magnitude for imperfect bonding conditions as compare to perfect bonding. On the contrary, in medium-II, stresses are greater in magnitude for imperfect bonding conditions as compare to perfect bonding. Also there is significant variations in magnitude of stresses for corresponding different bonding conditions in Medium-I as compare to medium-II. Also it is concluded that strain energy will transmit less in magnitude in Medium-I as stored energy density function is a linear function of strains and strains are proportionate to stresses. Stresses are transmitted from medium-II to Medium-I are less in magnitude and in view of this more energy will be conserved in medium-II due to imperfect bonding at interface.

APPENDICES

Appendix 1

Table 1: Source coefficients for numerous kind of seismic sources

Source	L_0	M_0	P_0	Q_0
Single couple (23) [direction of force is x_2 and arm is parallel to x_3]	$\mp\dfrac{\alpha_1 F_{23}}{2\pi}$	$\pm\dfrac{\alpha_1 F_{23}}{2\pi}$	0	0
Single couple(32) [direction of force is x_3 and arm is parallel to x_2]	$\pm\dfrac{\alpha_1 F_{32}}{2\pi}$	$\pm\dfrac{\alpha_1 F_{32}}{2\pi}$	0	0
double couple (23)+(32), moment of double couple is $F_{32}=F_{23}=D_{23}$	0	$\pm\dfrac{\alpha_1 D_{32}}{\pi}$	0	0
Center of rotation (32)-(23), $F_{32}=F_{23}=R_{23}$	$\pm\dfrac{R_{32}}{\pi}$	0	0	0
Dipole (22)	0	0	$\dfrac{(1-\alpha_1)F_{22}}{2\pi}$	$\dfrac{-\alpha_1 F_{22}}{2\pi}$
Dipole (33)	0	0	$\dfrac{(1-\alpha_1)F_{33}}{2\pi}$	$\dfrac{\alpha_1 F_{33}}{2\pi}$
Center of dilatation (22)+(33), $F_{22}=F_{33}=C_0$	0	0	$\dfrac{(1-\alpha_1)C_0}{\pi}$	0
Double couple (33)-(22), $F_{22}=F_{33}=D'_{23}$	0	0	0	$\dfrac{\alpha_1 D'_{23}}{\pi}$
Tensile dislocation in x_2-direction	0	0	$\dfrac{\alpha_1 T_0}{\pi}$	$\dfrac{-\alpha_1 T_0}{\pi}$
Tensile dislocation in x_3-direction	0	0	$\dfrac{\alpha_1 T_0}{\pi}$	$\dfrac{\alpha_1 T_0}{\pi}$
The upper and lower sign are for $z>\zeta$ and $z<\zeta$ resp., $\alpha_1 = \dfrac{\lambda_1+\mu_1}{\lambda_1+2\mu_1}$				

Appendix 2

$$E_1 = 2k_{33}(2\alpha_2\beta k_{22} + \alpha_1\alpha_2\beta^2 - \alpha_1\alpha_2\beta k_{22})/D$$

$$E_2 = 2k_{33}(\alpha_1\beta^2 - \alpha_2\beta k_{22} - \alpha_1\alpha_2\beta^2 + \alpha_1\alpha_2\beta k_{22})/D$$

$$F_1 = -2(\alpha_1\alpha_2\beta^2 k_{22} + \alpha_1\alpha_2\beta^2 k_{33})/D$$

$$F_2 = -2(\alpha_1\beta^2 k_{22} + \alpha_1\beta^2 k_{33} - \alpha_1\alpha_2\beta^2 k_{33} + \alpha_1\alpha_2\beta k_{22} k_{33})/D$$

$$F_3 = -2(-\alpha_1\alpha_2\beta^2 k_{22} + \alpha_1\alpha_2\beta^2 k_{33})/D$$

$$G_1 = (2\alpha_2\beta k_{22} - 2\alpha_2\beta k_{33} + \alpha_2{}^2\beta k_{22} + \alpha_2{}^2\beta k_{33} - 2\alpha_2{}^2 k_{22} k_{33} + \alpha_1\alpha_2{}^2\beta^2 + \alpha_1\alpha_2{}^2 k_{22} k_{33} - \alpha_1\alpha_2\beta k_{22} + \alpha_1\alpha_2\beta k_{33} - \alpha_1\alpha_2{}^2\beta k_{22} - \alpha_1\alpha_2{}^2\beta k_{33})/D$$

$$G_2 = (2\alpha_1\beta^2 + 2\alpha_2\beta k_{22} - 2\alpha_1\alpha_2\beta^2 + 2\alpha_1\alpha_2\beta k_{22})/D$$

$$G_3 = (2\alpha_2\beta k_{22} - 2\alpha_2\beta k_{33} + \alpha_2{}^2\beta k_{22} + 2\alpha_2{}^2\beta k_{33} - 2\alpha_2{}^2 k_{22} k_{33} + \alpha_1\alpha_2{}^2\beta^2 - \alpha_1\alpha_2\beta k_{22} + \alpha_1\alpha_2\beta k_{33} - \alpha_1\alpha_2{}^2\beta k_{22} - \alpha_1\alpha_2{}^2\beta k_{33} + \alpha_1\alpha_2{}^2 k_{22} k_{33})/D$$

$$H_1 = \alpha_2(2\alpha_2\beta k_{22} + 2\alpha_2\beta k_{33} - 4\alpha_2\beta k_{22} k_{33} + 2\alpha_1\alpha_2\beta^2 + 2\alpha_1\alpha_2\beta k_{22} - 2\alpha_1\alpha_2\beta k_{33} + 2\alpha_1\alpha_2\beta k_{22} k_{33})/D$$

$$H_2 = \alpha_2(\alpha_1\beta k_{22} - \alpha_2\beta k_{22} - \alpha_1\beta k_{33} - \alpha_2\beta k_{33} + 2\alpha_2 k_{22}\, k_{33} - \alpha_1\alpha_2\beta^2 + \alpha_1\alpha_2\beta k_{22} + \alpha_1\alpha_2\beta k_{33}$$
$$- \alpha_1\alpha_2 k_{22}\, k_{33})/D$$

$$H_3 = \alpha_2(2\alpha_2\beta k_{22} + 2\alpha_2\beta k_{33} - 4\alpha_2 k_{22}\, k_{33} + 2\alpha_1\alpha_2\beta^2 - 2\alpha_1\alpha_2\beta k_{22} - 2\alpha_1\alpha_2\beta k_{33}$$
$$+ 2\alpha_1\alpha_2 k_{22}\, k_{33})/D$$

and

$$D = \alpha_2(2\beta k_{22} + 2\beta k_{33} + 2\alpha_1\beta^2 - \alpha_1\beta k_{22} - \alpha_2\beta k_{22} - \alpha_1\beta k_{33} - \alpha_2\beta k_{33} + 2\alpha_2 k_{22}\, k_{33} - \alpha_1\alpha_2\beta^2$$
$$+ \alpha_1\alpha_2\beta k_{22} + \alpha_1\alpha_2\beta k_{33} - \alpha_1\alpha_2 k_{22}\, k_{33})$$

Appendix 3

For $z>0$;

$$\int_0^\infty \exp(-kz)\frac{sinky}{k}\,dk = tan^{-1}\frac{y}{z}$$

$$\int_0^\infty \exp(-kz)\frac{cosky}{k}\,dk = -2\ln(y^2 + z^2)$$

$$\int_0^\infty \exp(-kz)\,sinky\,dk = \frac{y}{y^2+z^2}$$

$$\int_0^\infty \exp(-kz)\,cosky\,dk = \frac{z}{y^2+z^2}$$

$$\int_0^\infty \exp(-kz)\,k\,sinky\,dk = \frac{2yz}{(y^2+z^2)^2}$$

$$\int_0^\infty \exp(-kz)\,k\,cosky\,dk = \frac{1}{y^2+z^2}\left[\frac{2z^2}{y^2+z^2} - 1\right]$$

$$\int_0^\infty \exp(-kz)\,k^2\,sinky\,dk = \frac{2y}{(y^2+z^2)^2}\left[\frac{4z^2}{y^2+z^2} - 1\right]$$

$$\int_0^\infty \exp(-kz)\,k^2\,cosky\,dk = \frac{2z}{(y^2+z^2)^2}\left[\frac{4z^2}{y^2+z^2} - 3\right]$$

$$\int_0^\infty \exp(-kz)\,k^3\,sinky\,dk = \frac{24yz}{(y^2+z^2)^3}\left[\frac{2z^2}{y^2+z^2} - 1\right]$$

$$\int_0^\infty \exp(-kz)\,k^3\,cosky\,dk = \frac{6}{(y^2+z^2)^2}\left[\frac{8z^4}{(y^2+z^2)^2} - \frac{8z^2}{y^2+z^2} + 1\right]$$

ACKNOWLEDGEMENT

REFERENCES

1. Dundurs, J. and Hete´nyi, M. (1965). "Transmission of Force Between Two Semi-Infinite Solids", *Journal of Applied Mechanics, Vol. 32, No. 3, pp. 671-674, https://doi.org/10.1115/1.3627277.*

2. Singh, S.J. and Garg, N.R. (1986). "On the Representation of Two-Dimensional Seismic Sources", *Acta Geophysica Polonica, Vol. 34, No. 1, pp. 1-12.*

3. Singh, S.J., Rani, S. and Garg, N.R. (1992). "Displacements and Stresses in Two Welded Half-Spaces Caused by Two-Dimensional Sources", *Physics of the Earth and Planetary Interiors, Vol. 70, No. 1-2, pp. 90-101. https://doi.org/10.1016/0031-9201(92)90164-Q.*

4. Yu, H.Y. (1998). "A New Dislocation-Like Model for Imperfect Interfaces and their Effect on Load Transfer", *Composites Part A 29A, pp. 1057–1062.*

5. Fan, H. and Wang, G.F. (2003). "Screw Dislocation Interacting with Imperfect Interface", *Mechanics of Materials, Vol. 35, No. 10, pp. 943-953, https://doi.org/10.1016/S0167-6636(02)00309-5.*

6. Singh, S.J. and Singh, M. (2004). "Deformation of a Layered Half-Space Due to a Very Long Tensile Fault", *Proceedings of the Indian Academy of Sciences, Earth and Planetary Sciences, Vol. 113, No. 2, pp. 235-246, https://doi.org/10.1007/BF02709790.*

7. Kumar, A., Singh, S.J. and Singh, J. (2005). "Deformation of Two Welded Elastic Half-Spaces Due to a Long Inclined Tensile Fault", *Journal of Earth System Science, Vol. 114, No. 1, pp. 97-103, https://Doi.Org/10.1007/BF02702012.*

8. Singh, K., Madan, D.K., Goel, A. and Garg, N.R. (2005). "Two-Dimensional Static Deformation of an Anisotropic Medium", *Sadhana-Acad, Proceedings Engineering Science, Vol. 30, No. 4, pp. 565-583, https://doi.org/10.1007/BF02703280.*

9. Bala, N. and Rani, S. (2009). "Static Deformation Due to a Long Buried Dip-Slip Fault in an Isotropic Half-Space Welded with an Orthotropic Half-Space", *Sadhana - Academy Proceedings in Engineering Sciences, Vol. 34, No. 6, pp. 887-902, https://doi.org/10.1007/s12046-009-0053-6.*

10. Chu, H.J., Pan, E., Han, X., Wang, J. and Beyerlein, I.J. (2012). "Elastic Fields of Dislocation Loops in Three-Dimensional Anisotropic Bimaterials", *Journal of the Mechanics and Physics of Solids, Vol. 60, No. 3, pp. 418-431, https://doi.org/10.1016/j.jmps.2011.12.007.*

11. Wu, W., Lv, C., Xu, S. and Zhang, J. (2017). "Elastic Field Due to Dislocation Loops in Isotropic Bimaterial with Dislocation-Like and Force-Like Interface Models", *Mathematics and Mechanics of Solids, Vol. 22, No. 5, pp. 1190-1204. https://doi.org/10.1177/1081286515622808.*

12. Kumari, A. and Madan, D.K. (2021). "Deformation Field Due to Seismic Sources with Imperfect Interface", *J. of Earth System Science, Vol. 130, No. 4, https://doi.org/10.1007/s12040-021-01712-0.*

13. Madan, D.K. and Kumari, A. (2022). "Stresses and Displacements for Two Imperfectly Joined Half-Spaces Induced by Vertical Tensile Fault", *Proceedings of the Indian National Science Academy, Vol. 88, No. 1, pp. 104-115, https://doi.org/10.1007/s43538-021-00060-3.*